Computers, Materials & Continua

Tech Science Press

Doi:10.32604/cmc.2025.070222

ARTICLE

An Optimal Right-Turn Coordination System for Connected and Automated Vehicles at Urban Intersections

Mahmudul Hasan[1], Shuji Doman[1], A. S. M. Bakibillah[2], Md Abdus Samad Kamal[1,*] and Kou Yamada[1]

[1]Department of Mechanical Science and Technology, Graduate School of Science and Technology, Gunma University, Kiryu, 376-8515, Japan

[2]Department of Systems and Control Engineering, School of Engineering, Institute of Science Tokyo, Tokyo, 152-8552, Japan

*Corresponding Author: Md Abdus Samad Kamal. Email: maskamal@gunma-u.ac.jp

Received: 10 July 2025; Accepted: 10 October 2025; Published: 10 November 2025

ABSTRACT: Traffic at urban intersections frequently encounters unexpected obstructions, resulting in congestion due to uncooperative and priority-based driving behavior. This paper presents an optimal right-turn coordination system for Connected and Automated Vehicles (CAVs) at single-lane intersections, particularly in the context of left-hand side driving on roads. The goal is to facilitate smooth right turns for certain vehicles without creating bottlenecks. We consider that all approaching vehicles share relevant information through vehicular communications. The Intersection Coordination Unit (ICU) processes this information and communicates the optimal crossing or turning times to the vehicles. The primary objective of this coordination is to minimize overall traffic delays, which also helps improve the fuel consumption of vehicles. By considering information from upcoming vehicles at the intersection, the coordination system solves an optimization problem to determine the best timing for executing right turns, ultimately minimizing the total delay for all vehicles. The proposed coordination system is evaluated at a typical urban intersection, and its performance is compared to traditional traffic systems. Numerical simulation results indicate that the proposed coordination system significantly enhances the average traffic speed and fuel consumption compared to the traditional traffic system in various scenarios.

KEYWORDS: Right-turn coordination; connected and automated vehicles; vehicular communication; edge processing; urban intersection

1 Introduction

In the past few decades, widespread traffic congestion has affected many major cities in developed nations. Key factors contributing to traffic congestion include increasing urbanization, unplanned transport infrastructure, inadequate public transport systems, heavy traffic flow in single lanes with short-distance crossings, and the rising number of personal vehicles [1]. Moreover, a vehicle's right turn on a single-lane road, considering left-hand side driving (equivalently, left turn in the context of right-hand side driving of the roads), often causes congestion and consequently delays the movement of following vehicles. This congestion disrupts the smooth flow of traffic because oncoming vehicles usually do not yield to the right-of-way until the traffic signal changes from green to red, causing significantly increased delays, fuel consumption, and emissions during traffic congestion [2]. Studies show that vehicle energy consumption increases considerably due to frequent stopping, starting, and idling at intersections [3]. Moreover, turning-related accidents account for a large portion of intersection crashes. Therefore, developing control systems

to enhance the coordination of turning vehicles at intersections is crucial for reducing accidents, delays, and fuel consumption.

In the emerging paradigm of connected and automated transportation, Vehicle-to-Everything (V2X) communication is expected to play a crucial role in enhancing road safety, improving traffic efficiency, and enhancing passenger infotainment [4]. Existing Dedicated Short-Range Communications (DSRC)-based V2X technology and emerging cellular-based V2X technologies, when combined with cloud-based fast computing facilities, can be utilized to create efficient traffic coordination systems. These V2X technologies can establish a cyber-physical framework that facilitates effective coordination between vehicles and traffic lights at intersections [5]. Numerous studies have proposed systems for the optimal coordination of connected and automated vehicles [6]. Miculescu and Karaman [7] proposed an algorithm for coordinated control of autonomous vehicles at intersections without signals. They demonstrate how a polling system can be utilized to coordinate communication and behavior among vehicles, thereby achieving safe and efficient traffic flow at intersections. The framework aims to coordinate and optimize vehicle traffic on multi-lane highways, leveraging advanced sensor technology and real-time data analysis. There are also extensive works on adaptive signal control and traffic coordination in connected vehicle environments. For example, Li et al. [8] reviewed adaptive signal control and its effects on urban traffic. It described how connected vehicles can dynamically adjust traffic signals to reduce traffic congestion.

Additionally, studies are being conducted on the application of communication technologies at smart intersections. Namazi and Taghavipour [9] investigated the use of Vehicle-to-Vehicle (V2V) and Vehicle-to-Infrastructure (V2I) communication systems to enhance traffic flow and reduce emissions. This research demonstrates how real-time communication between vehicles and infrastructure can be utilized to efficiently manage traffic and reduce emissions at intersections. Galvão et al. [10] proposed a method to optimize the management of urban intersections using visible light communications. This approach aimed to enhance traffic flow and minimize delays at intersections by coordinating the control of vehicles and traffic signals. Other studies proposed distributed routing systems in urban areas using Vehicular Ad-hoc Networks (VANETs) [11]. Particularly, they presented an innovative approach to optimizing urban traffic flow in real-time at signalized intersections, and Wang et al. [12] proposed an augmented vehicle-following model at unsignalized intersections. The models aimed to achieve safe and efficient traffic flow by coordinating vehicle movements based on V2V communication.

Some studies analyzed the intersection control of autonomous vehicles using Model Predictive Control (MPC). Farkas et al. proposed algorithms that allow autonomous vehicles to operate safely and efficiently at intersections [13]. Xu et al. [14] proposed a method for coordinating signal optimization and speed control at isolated intersections. The method aims to optimize traffic flow by enabling connected vehicles to control signals and speeds at intersections cooperatively. Yang et al. [15] designed human-machine interfaces that provide right-turn timing at intersections. They evaluated the effectiveness of the interface in providing drivers with appropriate right-turn timing. Sun et al. [16] studied interactive left turns by automated vehicles at uncontrolled intersections. This research investigated how automated vehicles can safely interact with other vehicles during left turns. Mahler and Vahidi [17] proposed a method for probabilistically predicting traffic signal timings and optimizing vehicle velocity based on these predictions. These studies contribute to energy efficiency and emphasize the importance of eco-driving, taking into account traffic signals and road conditions. Bento et al. [18] study the environmental impact of intelligent vehicle control at intersections via V2V and V2I communication. This study examines the environmental implications of intelligent vehicle control at intersections and demonstrates how efficient traffic management can mitigate environmental impacts. Existing works on intersections mainly focused on signal control or trajectory

control of approaching vehicles (partially or fully connected) at the intersection. However, the right-turn coordination of CAVs at intersections did not receive much attention.

In this study, we developed an optimal right-turn coordination system for CAVs at single-lane intersections. It is assumed that under a Level 3 autonomous driving system, or Conditional Driving Automation [19], enabling a vehicle to drive itself under specific conditions and within limited areas, provided the driver is ready to retake control when the system requests it. Such a driving system can automatically adjust the speed according to the target crossing time given by the ICU, using the V2V communication system. The right-turn vehicle and the vehicles in the opposite lane are optimized to follow a target trajectory for a smooth right turn. In this study, the number of right-turning vehicles is considered insignificant, and therefore, no right-turn lanes or right-turn signal phases are installed. The right-turning vehicle and oncoming vehicles measure the time from their current position to reach the intersection and share that time, allowing the oncoming vehicle to decide whether to yield to the right-turning vehicle. We set a time interval to ensure a safe right turn, thereby avoiding a collision between the right-turning vehicle and the oncoming vehicle. It is found that the system minimizes the objective function in terms of overall delay time due to right turns, thereby improving traffic flow and fuel consumption.

2 Methodology

This section presents a comprehensive methodology for the proposed system. It begins with the problem statement, vehicle dynamics, and models of traditional driving. The typical decision-making process for right turns is analyzed, followed by the design of a cyber-physical optimal coordination framework where vehicles communicate with an Intersection Coordination Unit (ICU) via V2X technologies. For convenience, the key variables and parameters are summarized in Table 1.

Table 1: List of key symbols used in the models proposed in this paper

Symbol	Description	Symbol	Description
x_n, v_n	Position and velocity (of vehicle n)	a_n	Acceleration of vehicle (control input)
l_n	Length of vehicle	Δt	Simulation time step size
v_d, T	Desired velocity and time gap	R_0	Minimum gap at stop
b	Comfortable deceleration	a	Maximum acceleration
X_{stop}	Stopping point before intersection	l_{stop}	Distance to stopping point
W_{rtp}	Length of right-turn path	W_{tdz}	Width of turning decision zone
μ_o	Coefficients of velocity estimation function	θ_n	Feasibility of right turn (binary)
$\bar{\tau}_{em}, \bar{\tau}_{wm}$	Estimated arrival time of mth e (East) and w (West) vehicle	τ_{em}, τ_{wm}	Coordinated arrival time of mth e (East) and w (West) vehicle
τ_{safe}	Safety threshold time for crossing	h_{time}	Safe car-following time headway
$\Delta\tau$	Time step for arrival time estimation	b_i, c_i	Fuel consumption model coefficients

2.1 Problem Statement

In the context of road traffic systems in Japan, let us consider a typical single-lane urban intersection without an auxiliary short right-turning lane or a dedicated turning signal phase, due to a small volume of turning traffic. In a green phase, a vehicle can turn right only if there is a safe gap between a pair of vehicles in the opposite lane or wait until the end of the red phase (i.e., turn in the inter-phase time). When a vehicle fails to turn smoothly at such intersections in relatively dense traffic, it often blocks many straight-going vehicles

behind it, leading to severe congestion, as illustrated in Fig. 1. Coordinating a large number of vehicles from a distance optimally is not feasible in such critical scenarios due to the complexity of the required computations and communication, as well as the necessary safety concerns. Therefore, a limited centralized coordination followed by fully distributed local control is the best solution, as considered in this paper. In this study, we assume an upcoming scenario in which all vehicles communicate their states and turning intentions to the ICU upon arrival within the communication range. It is also assumed that the communication is ideal, with no significant delay, and the ICU has a proper sensing method to detect any pedestrian crossing, thereby constraining the turning time in the optimization to avoid a potential accident. The problem considered for the ICU is to optimally determine the safe turning and crossing times of all vehicles, thereby minimizing the overall traffic delay and coordinating vehicles efficiently.

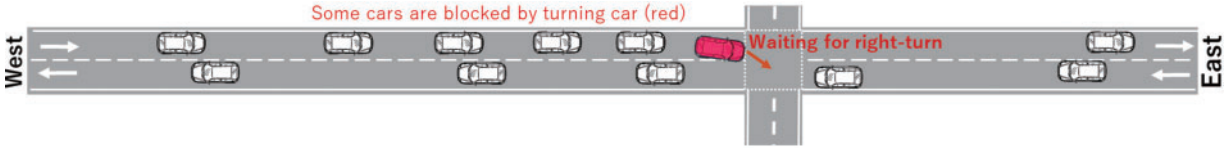

Figure 1: Typical traffic congestion created by right-turn delays as a car (red) from the West waits to turn, causing many cars behind to wait for a longer period

2.2 Vehicle Dynamics and Motion Control

For the development of a new traffic coordination system, the traditional vehicle control with turning decisions at the intersection is modeled first. The dynamic behavior related to the longitudinal motion of a vehicle is the basis of this study, where the position x_n, velocity v_n, and acceleration a_n of any vehicle n at discrete time t with step size Δt are expressed as

$$x_n(t+1) = x_n(t) + v_n(t)\Delta t + 0.5a_n(t)\Delta t^2, \tag{1}$$

$$v_n(t+1) = v_n(t) + a_n(t)\Delta t. \tag{2}$$

The primary driving task is determining the control input $a_n(t)$ based on the traffic flow, signal status, and road conditions. For typical human driving, a time-continuous car-following model called the Intelligent Driver Model (IDM) is employed in this study to simulate traffic conditions under traditional scenarios [20]. Typically, the acceleration of vehicle n can be obtained using the state of the vehicle and its preceding vehicle or traffic signal, which can be given as

$$a'_n(t) = f_{\text{cf}}(x_n(t), v_n(t), x_{n-1}(t), v_{n-1}(t)). \tag{3}$$

Using the IDM, the car-following function f_{cf} is defined as

$$f_{\text{cf}}(x_n, v_n, x_{n-1}, v_{n-1}) = a\left(1 - \left(\frac{v_n}{v_d}\right)^4 - \left(\frac{R_0 + v_n T + v_n(v_n - v_{n-1})/2\sqrt{ab}}{x_{\text{n-1}} - x_n - l_n}\right)^2\right), \tag{4}$$

where variables l_n, v_d, R_0, T, a, and b represent the vehicle length, target velocity, minimum distance between vehicles, target time gap between vehicles, maximum acceleration, and minimum comfortable deceleration, respectively.

The IDM can regulate the acceleration of a vehicle based on its position and velocity; however, it cannot directly incorporate the effects of traffic signals or turning points where a car must stop first. Therefore, for any target stopping point X_{stop} ahead (e.g., due to a red signal or safety confirmation before turning), a

data-driven model is adopted to describe a vehicle motion closely approaching a red signal [21]. Specifically, the velocity as a polynomial function of distance-to-stop l_{stop} for $l_{\text{stop}} \le L_{\text{th}}$ is obtained from experimental driving data as

$$v_n^*(l_{\text{stop}}) = \sum_{o=1}^{\mathcal{O}} \mu_o l_{\text{stop}}^o, \tag{5}$$

where, based on experimental driving data fittings, the order of polynomial fittings is $\mathcal{O} = 5$, and coefficients μ_o are obtained as $\mu_5 = 5.635 \times 10^{-10}$, $\mu_4 = -3.446 \times 10^{-7}$, $\mu_3 = +7.925 \times 10^{-5}$, $\mu_2 = -8.519 \times 10^{-3}$, and $\mu_1 = 0.4805$.

Using $v_n^*(l_{\text{stop}})$ in (5) and its derivative $dv_n^*(l_{\text{stop}})/dl_{\text{stop}}$, the acceleration (or deceleration) of any vehicle n with a velocity v_n and stopping distance $l_{\text{stop}} = X_{\text{stop}} - x_n$ towards a complete stop can be estimated as

$$f_{\text{stop}}(x_n, v_n, X_{\text{stop}}) = \frac{v_n^2}{v_n^*(l_{\text{stop}})} \times \left(\frac{\mathrm{d}v_n^*(l_{\text{stop}})}{\mathrm{d}l_{\text{stop}}} \right). \tag{6}$$

Since the model is valid only for a limited distance $l_{\text{stop}} \le L_{\text{th}}$, the acceleration of a vehicle approaching the intersection is obtained as

$$a_n''(t) = \begin{cases} f_{\text{stop}}(x_n(t), v_n(t), X_{\text{stop}}), & \text{if } X_{\text{stop}} - x_n(t) \le L_{\text{th}}, \\ f_{\text{cf}}(x_n(t), v_n(t), X_{\text{stop}}, 0), & \text{otherwise.} \end{cases} \tag{7}$$

In (7), for the case $l_{\text{stop}} > L_{\text{th}}$, the car-following model in (4) is used with a target to stop at the intersection stopping point. In the event of a green signal for a straight-going vehicle, X_{stop} is assumed to be infinitely large (i.e., $X_{\text{stop}} = \infty$). Finally, the acceleration of a vehicle n for safe driving is given as

$$a_n(t) = \min(a_n'(t), a_n''(t)), \tag{8}$$

which ensures collision-free stopping behavior of vehicle n for any unsafe gap with the preceding vehicle $n-1$ under all circumstances.

2.3 Typical Right-Turning Decision

Here we explain a vehicle's typical right-turning decision process using the illustration in Fig. 2, where vehicle n (shown in red) from the West has to turn right, and others are straight-going vehicles. It approaches the intersection stop point X_{stop} and stops completely if a safe gap with vehicles from the East is insufficient. However, when the vehicle is in the *turning decision zone* (tdz) of a length W_{tdz} (from X_{stop}), it can estimate the safe passage between the opposite vehicle pair ($m-1$ and m from the East as shown in Fig. 2) and executes turning by following the standard *right turn path* (rtp) shown by the arrow of a length W_{rtp} at the intersection. We assume a binary variable $\theta_n(t) = 0$ represents the vehicle position at $x_n(t) \in [X_{\text{stop}} - W_{\text{tdz}}, X_{\text{stop}}]$ is not in a feasible or safe state for turning execution over the intersection, which is defined as

$$\theta_n(t) = \begin{cases} 1 & \text{if } (\bar{\tau}_{em} - \bar{\tau}_{wn} > \tau_{\text{safe}}) \text{ and } (\bar{\tau}_{wn} - \bar{\tau}_{e(m-1)} > \tau_{\text{safe}}), \\ 0 & \text{if } x_n(t) < X_{\text{stop}} - W_{\text{tdz}} \text{ or } x_n(t) > X_{\text{stop}} + W_{\text{rtp}}, \end{cases} \tag{9}$$

where $\bar{\tau}_c,\ c \in \{wn, em, e(m-1)\}$ is the estimated time to cross the point $X_{\text{stop}} + W_{\text{rtp}}$ and τ_{safe} is a safety threshold for crossing. For the right turning vehicle n with $\theta_n(t) = 0$ approaching to stop at X_{stop}, change its path to execute the turning process when $\theta_n(t) = 1$, which is reset again once it passes beyond $X_{\text{stop}} + W_{\text{rtp}}$.

At a signalized intersection, the inter-phase time (at the end of the green signal) often provides a sufficient gap (for a large $\tilde{\tau}_{em}$), and a vehicle can execute the turning. However, any vehicles waiting behind must wait for at least the red period before passing through the intersection in the next cycle. In dense traffic conditions, such a right-turning vehicle at the leading part of a queue may trigger spillback congestion. Therefore, it is desired to coordinate all vehicles to ensure smooth traffic flows, which is described in the next section.

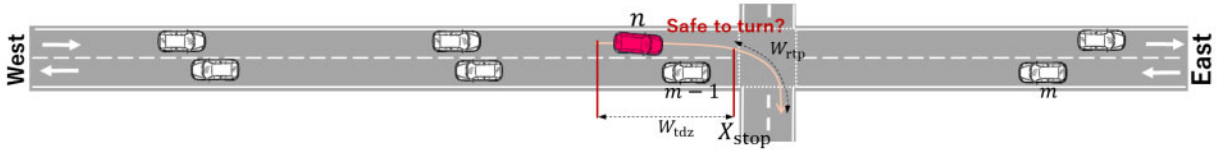

Figure 2: Typical right-turn decision process by a vehicle (red) in the decision zone that evaluates expected safe gaps with conflicting vehicles $m-1, m$ from the East

2.4 Proposed Intersection Coordination System

Fig. 3 illustrates the schematic diagram of the proposed optimal coordination system under a cyber-physical framework. We assume a connected vehicle environment under a VANET around the intersection with a communication zone of range d_{cz}, where vehicles transmit their states and turning intention to the roadside ICU using V2I communication and receive individualized coordination signals using I2V communication. At the ICU cyber level, edge processing is carried out to determine the optimal turning and crossing times for all vehicles from both directions, minimizing an objective function while satisfying signal-relevant rules, ensuring safety, and promoting user comfort. In particular, vehicle states, turning information, and signal-phase-and-timing (SPaT) information are used to predict the natural trajectory of the vehicles using some models. Then, the optimization of trajectories incorporating turning time is performed at the start of a green signal. The optimal timing for each vehicle is fed back to them through I2V communication, as shown in Fig. 3. It is assumed that an automated driving system or a driver with an assistance system controls each vehicle adequately.

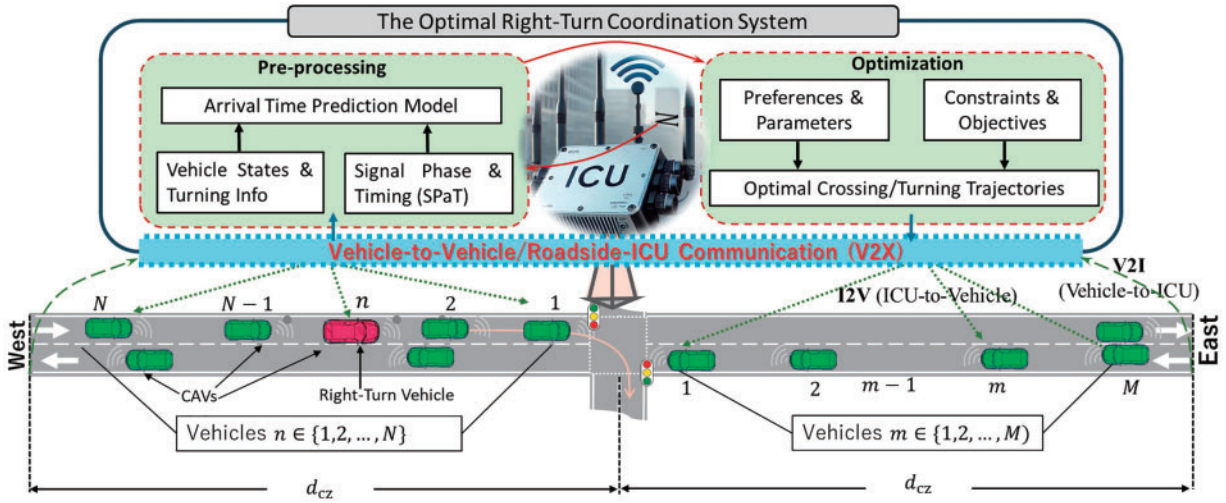

Figure 3: Schematic diagram of the cyber-physical optimal right-turn coordination system at an intersection, which includes all CAVs sharing information with ICU

2.5 Optimal Right-Turn Coordination Decision

To reduce total delay time for all vehicles at an intersection, right-turning vehicles and incoming traffic from opposite directions should adjust their spacing and velocity efficiently. The optimal right-turn coordination system receives necessary information from vehicles approaching the intersection, computes the best driving strategy considering the right-turn vehicles, and communicates this strategy to individual vehicles. Then, the local controller of each automated vehicle executes this driving strategy, ensuring it satisfies safety constraints on the road. The optimal right-turn coordination system plans when to execute the right turn.

We assume that among vehicles $\mathcal{V}_{\text{West}} = \{1, 2, \ldots, N\}$ from the West, the n-th vehicle has to turn right, considering a safe gap between a suitable pair of $m-1$ and m vehicles among $\mathcal{V}_{\text{Eest}} = \{1, 2, \ldots, M\}$, or after the M-th one, i.e., $M+1$ arriving from the East. At any initial vehicle state at the start of a green phase, the natural or unconstrained arrival times of vehicles for crossing the intersection from the East and the West are defined as $\tau_{\text{em}} = [\tau_{\text{e1}}, \tau_{\text{e2}}, \ldots, \tau_{\text{e}M}]^\top \in \mathbb{R}^M$ and $\tau_{\text{wn}} = [\tau_{\text{w1}}, \tau_{\text{w2}}, \ldots, \tau_{\text{w}N}]^\top \in \mathbb{R}^N$, respectively. The aim is to find the optimal $p^* \in \{1, 2, \ldots, M, M+1\}$ as the relative position (concerning one of m vehicles) where a vehicle $q \in \mathcal{V}_{\text{West}}$ from the West should execute turning safely based on the optimal crossing times $\tau^*_{\text{wn}}, \tau^*_{\text{em}}$ by minimizing an objective function and typical driving safety constraints. Specifically, $p^* = 2$ indicates that vehicle q is allowed to turn before vehicle $m = 2$ (after vehicle $m = 1$), and $p^* = M+1$ implies that vehicle q should turn after vehicle $m = M+1$ from the East. We consider the following quadratic objective function in terms of the anticipated delay $(\bar{\tau}_{..} - \tau_{..})$ of each vehicle for a given turning path defined by p as

$$J(p, \tau_{\text{wn}}, \tau_{\text{em}}) = \omega_{East} \sum_{m=p}^{M} (\bar{\tau}_{em} - \tau_{em})^2 + \omega_{West} \sum_{n=q}^{N} (\bar{\tau}_{\text{w}n} - \tau_{\text{w}n})^2, \tag{10}$$

where ω_{East} and ω_{West} are constant weights used to softly adjust the priority by tuning the values to reflect the relative cost of delay for cars from the East and the West. Note that vehicles 1 to $q-1$ from the West and 1 to $p-1$ from the East move without interruption and are excluded from the objective function since their delay time is zero. The car-following vehicles on the same path must have a safe gap with others, and the turning vehicle (from the West) must find a sufficient safe gap between the two vehicles from the East. Considering such constraints, the optimal coordination task is defined as the solution $p^*, \tau^*_{\text{w}}, \tau^*_{\text{e}}$ of the objective function given by

$$\min_{p, \tau_{\text{wn}}, \tau_{\text{em}}} J(p, \tau_{\text{wn}}, \tau_{\text{em}}) \tag{11}$$

subject to

$$\begin{aligned}
&\tau_{em} = \bar{\tau}_{em}, \ m = 1, 2, \ldots, p-1, \\
&\tau_{\text{w}n} = \bar{\tau}_{\text{w}n}, \ n = 1, 2, \ldots, q-1, \\
&\tau_{\text{w}q} = \max(\tau_{\text{e(p-1)}} + \tau_{\text{safe}}, \ \bar{\tau}_{\text{w}q}), \\
&\tau_{ep} = \max(\tau_{\text{w}q} + \tau_{\text{safe}}, \ \bar{\tau}_{ep}), \\
&\tau_{em} = \max(\tau_{\text{e}(m-1)} + h_{\text{time}}, \ \bar{\tau}_{em}), \quad m = q+1, q+2, \ldots, M, \\
&\tau_{\text{w}n} = \max(\tau_{\text{w}\,(n-1)} + h_{\text{time}}, \ \bar{\tau}_{\text{w}n}), \quad n = p+1, p+2, \ldots, N,
\end{aligned} \tag{12}$$

where h_{time} is the safe car-following time headway, which is determined considering a typical saturation flow rate, as $h_{\text{time}} = 2$ s. Note that the above optimization problem can also be extended to multiple right-turning vehicles per cycle by applying it successively to optimize the first turning vehicle, then the second, considering only those natural arrivals that are affected, and so on. Such an approach only requires the selection of those vehicles in the optimization framework, without changing this formulation. This optimization problem is

solved at the beginning of each green phase, considering all vehicles anticipated to arrive at the intersection before the onset of the red phase. The individual vehicles are given the target crossing and turning time using I2V communication to adjust their speed accordingly. After this initial coordination, the vehicles are controlled in a distributed manner, enabling safe operation in accordance with local conditions.

2.6 Estimation of Arrival Time

In the above optimization problem, the free flow arrival times, $\bar{\tau}_{em}, m \in \mathcal{V}_{East}$, and $\bar{\tau}_{\mathrm{wn}}, n \in \mathcal{V}_{West}$ for crossing the intersection need to be estimated once at the beginning of a green phase, when the vehicles may have different position and velocity along the road, i.e., traveling at a constant speed is very unlikely. Therefore, an interactive approach to estimating vehicle arrival times is considered. Specifically, with a discrete time frame $k = 0, 1, 2, 3, \ldots, K$ with a step size $\Delta\tau$, the arrival time of a vehicle $i \in \{m, n\}$ from $\psi \in \{\mathrm{e}, \mathrm{w}\}$ at stop point X_{stop} of the intersection is given as

$$\bar{\tau}_{\psi i} = \max\left(K\Delta\tau, \bar{\tau}_{\psi(i-1)} + h_{\mathrm{time}}\right), \tag{13}$$

where K is the final step in the iterative process, with the relationship given as

$$\bar{z}_i(K-1) < X_{\mathrm{stop}} \leq \bar{z}_i(K), \tag{14}$$

subject to, with $\bar{z}_i(0) = x_i(0), \bar{v}_i(0) = v_i(0)$,

$$\begin{aligned} \bar{z}_i(k+1) &= \bar{z}_i(k) + \bar{v}_i(k)\Delta\tau + 0.5a_i(k)\Delta\tau^2, \\ \bar{v}_i(k+1) &= \bar{v}_i(k) + a_i(k)\Delta\tau, \end{aligned} \tag{15}$$

for $k = 0, 1, 2, \ldots, K$. The acceleration $a_i(k)$ is determined based on (3) if the vehicle goes straight without slowing down, and when the vehicle needs to slow down or stop due to a right turn, a data-driven acceleration model is used according to [21] as

$$a_i(k) = \begin{cases} f_{\mathrm{ss}}(v_i, X_{\mathrm{stop}} - x_i) & \text{for stopping} \\ f_{\mathrm{cf}}(x_i, v_i, x_\infty, v_d) & \text{otherwise.} \end{cases} \tag{16}$$

Finally, the overall functional flowchart is shown in Fig. 4, including the safe driving process of individual vehicles and the cooperating process with the ICU.

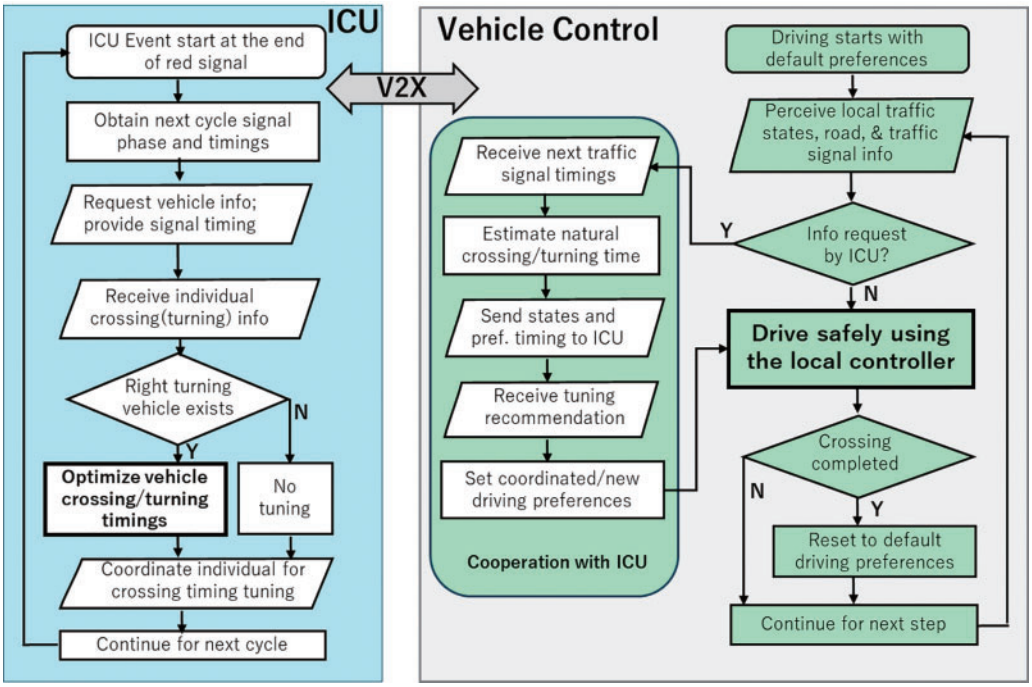

Figure 4: Functional flowchart showing ICU coordination process, basic driving decision of individual vehicles, including cooperation process with ICU

3 Results and Discussion

The proposed right-turn coordination system is assessed using microscopic simulation methods. The evaluation includes the proposed arrival prediction model, followed by an assessment of the proposed system under typical implemented scenarios that incorporate microscopic trajectories and individual driving behaviors. Finally, the impact of traffic variation is compared to the overall average traffic performance. The discussion surrounding the proposed system, including its limitations, computational complexity, implementation challenges, and potential for future enhancements, is described.

3.1 Simulation Settings

To evaluate the proposed right turn coordination system, a microscopic traffic simulation framework is built in MATLAB, as in Fig. 2, where a 1 km road features an intersection at 500 m, and has a speed limit of 50 km/h. The route is single-lane and allows vehicles to turn right at the intersection. Traffic lights are set at 40 s each for red and green signals, with an 80 s cycle. The traffic flow volume is set at a moderate level, and the parameters of the car-following model are chosen typically to reflect typical human driving behavior. The safe car-following time gap h_{time} and right turning gap are set as 2 and 4 s, respectively. For slowing down due to turning or stopping at a red signal, the maximum length is set at L_{th} = 180 m from the intersection, based on the experimental driving data fitting model. The weights ω_{East} and ω_{West} are set to 1 for equal priority in this study.

The fuel consumption rate f for a typical vehicle i can be obtained using an arbitrary velocity v_i and acceleration a_i as follows [22]

$$f = b_0 + b_1 v_i + b_2 v_i^2 + b_3 v_i^3 + \bar{a}_i (c_0 + c_1 v_i + c_2 v_i^2), \tag{17}$$

where $\bar{a}_i = a_i$ for $a_i > 0$ otherwise $\bar{a}_i = 0$ (for braking) and the fuel consumption parameters for a typical car are set as $b_0 = 0.1569$, $b_1 = 2.450 \times 10^{-2}$, $b_2 = -7.415 \times 10^{-4}$, $b_3 = 5.975 \times 10^{-5}$, $c_0 = 0.07224$, $c_1 = 9.681 \times 10^{-2}$, $c_2 = 1.075 \times 10^{-3}$. It is presumed that no fuel is consumed while braking, i.e., $a_i \leq 0$ from a high speed.

First, we demonstrate the estimation of arrival/crossing times of vehicles at the intersection using (16), to show that for any initial velocity and distance (to the crossing point of the non-turning vehicle), it can estimate the required arrival time (in the absence of a nearby preceding vehicle). Particularly, we choose arbitrary distances to the intersection and velocity (represented by a black circle) to estimate a vehicle's predicted natural arrival time and associated velocity patterns. Fig. 5a depicts the sample velocity profiles with estimated arrival/crossing times of vehicles at the intersection for freely traveling in a green signal, and Fig. 5b depicts the same in the case of slowing or stopping (due to turning or a red signal). Specifically, the time is calculated in seconds using the velocity curves from the black circle to the intersection crossing point at 500 m, and the corresponding velocity profile is displayed for each case. It is found that the estimated arrival times mostly closely match the measured arrival times for uncontrolled cases. These estimated values in $\bar{\tau}_{\psi i}$ are utilized to estimate a vehicle's delay and evaluate parameters to optimize the objective function and determine the optimal turning coordination.

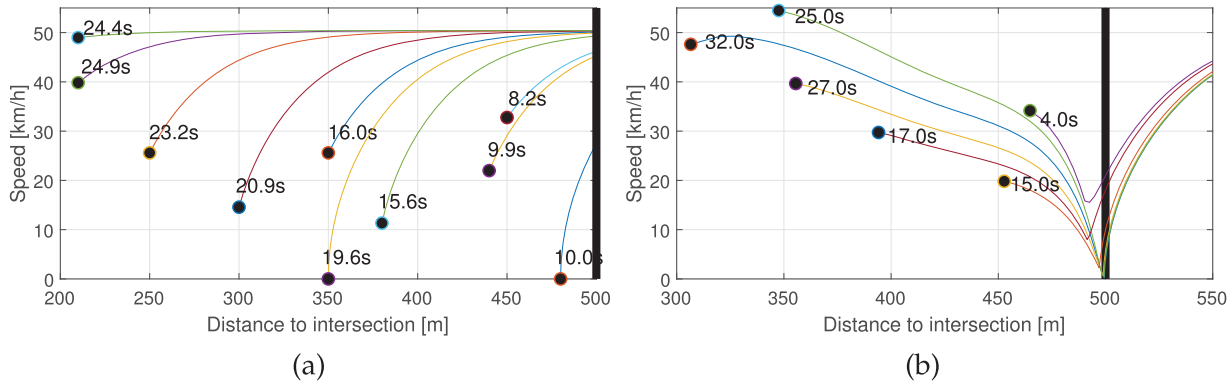

Figure 5: Example of predicted arrival times estimated for different speeds and distances shown by black circles based on speed profiles along the road (the thick vertical line shows the intersection position): (**a**) when vehicles travel freely during a green signal and (**b**) when vehicles must slow down or stop for a red signal

3.2 Evaluation of the Proposed Method

For simplicity, we consider that the signal becomes green at simulation time 0. Eleven vehicles from the West and eight vehicles from the East approach the intersection from some random positions. The fifth one from the West is set as a turning vehicle. In this case, the uncoordinated traditional traffic is first simulated, and the trajectories of the East and the West cars are displayed in Fig. 6a,b, respectively. For clarity, the traffic light is depicted with a white dashed line on each side, indicating the precise center of the intersection, and the vehicles are numbered in order of arrival. In Fig. 6, the 5th vehicle, indicated in red, slows down when approaching the intersection and eventually stops while looking for a safe gap. The vehicles from the East (represented in blue solid lines) do not create a gap for the turning vehicle from the West because they have a greater presence or priority. Finally, it executes the turning maneuver when all eight vehicles from the East cross the intersection. The 6th to 11th vehicles from the West take extra time to cross afterward. The trajectory of the West vehicles (Fig. 6b) shows that the 7th to 11th vehicles have to stop at the red signal for about 40 to 80 s.

This is because the vehicles to the East (Fig. 6a) do not consider the right-turning vehicle and pass through the intersection without slowing down. This extra delay of some vehicles may create spill-back

congestion with the same green duration. To avoid such a delay, the signal cycle is typically made longer in the traditional system, resulting in extra idling of other phase vehicles during the red phase.

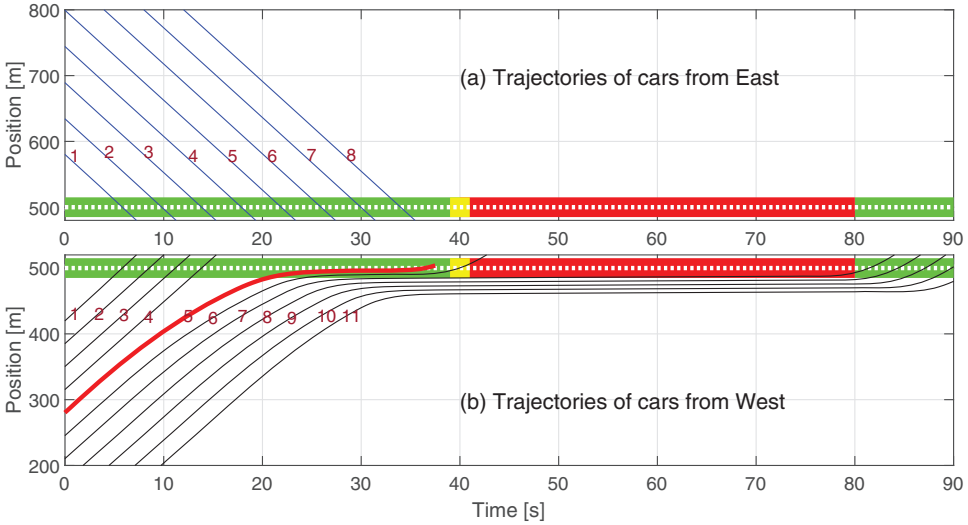

Figure 6: Traffic signals at intersection at 500 m, and trajectories of vehicles from both sides: (**a**) the East and (**b**) the West, with the Human Driving Model. East vehicles (blue) cross straightaway while the turning vehicle (5th, with thick-red) forces others behind to idle until the next green

In contrast, Fig. 7 shows the trajectory of the vehicles under the proposed coordination scheme. Based on optimal coordination at the beginning of green time, each vehicle is assigned its desired optimal crossing or turning time, which reduces the total delay in a quadratic sense, as defined by the objective function. The optimal $p^* = 5$ is found to be a solution that creates a gap between the 4th and 5th vehicles from the East, and the 5th vehicle from the West arrives in a way that allows it to turn at a comparatively higher speed without waiting. Consequently, the rest of the vehicles from the West also cross the intersection within the green time, with little impact on the East vehicles. Therefore, such coordination can accommodate all vehicles within the given 40 s green time. Comparing the velocity of the 5th vehicle in both cases (Figs. 6 and 7), with coordination, the right-turning vehicle turns the intersection at a velocity of about 24 km/h, much higher than about 4 km/h without coordination. Such a low velocity drop also indicated better fuel-efficient driving.

Fig. 8a shows the average speed of these vehicles for both sides, and the corresponding mean speed using solid lines. The 5th and its follower from the East side slightly reduce their speed under coordination to facilitate the smooth turning of the 5th vehicle from the West side. Such a slight drop in velocity significantly increases the speed of many vehicles in the West. Considering only the affected vehicles from both sides (i.e., the 5th–8th from the East and 5th–11th from the West), the average speed for the proposed coordinated system is 35.62 km/h, significantly higher than that of traditional systems, which average 24.76 km/h.

Fig. 8b shows the corresponding fuel consumption of the vehicles and the average values for each side under both schemes. The fuel consumption of the 5th and its followers from the East under the coordinated scheme tends to increase compared to the traditional case because they adjust their acceleration to allow more space for the right turn, which increases fuel consumption, albeit only slightly. However, the fuel consumption of the vehicles in the West (Fig. 8 right side) is significantly reduced compared to the East vehicles. The total fuel consumption of the vehicles in both lanes affected by the right-turning vehicles was 228.5 mL for the traditional driving system and 171.1 mL for the proposed coordinated driving system, resulting in a 25.12% reduction in overall fuel consumption.

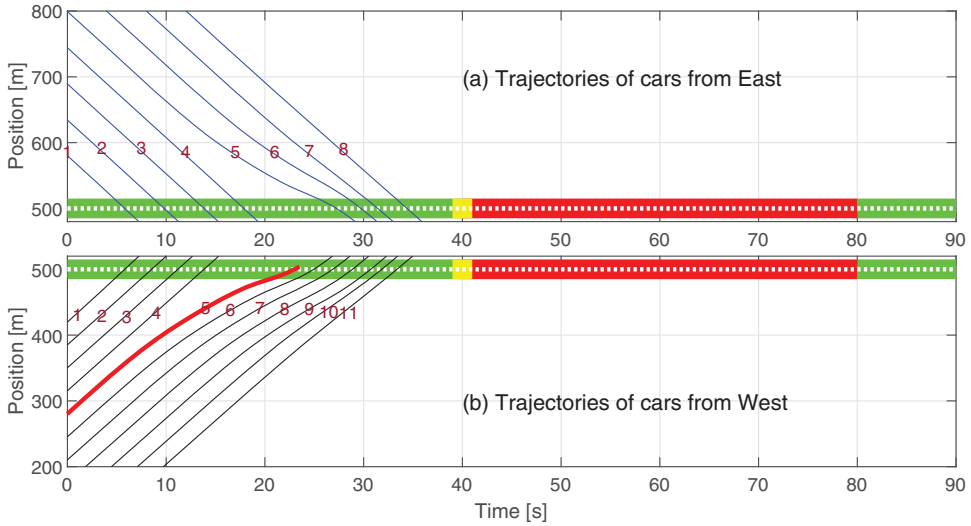

Figure 7: Traffic signals at intersection at 500 m, and trajectories of vehicles from both sides: (**a**) the East and (**b**) the West, the proposed optimized driving system. Trajectories show all vehicles from both sides passing before the red signal

Fig. 8 shows the velocity and fuel consumption of the first four vehicles from the West, and four from the East are unchanged in both cases, as they are not affected by the right turning of the 5th vehicle. Therefore, the overall performance is investigated as it varies depending on the position of the turning vehicle from the West. Fig. 9 shows the average traffic velocity and fuel consumption of all vehicles from both sides using markers under the schemes for the position of the turning vehicle in the queue. When it is in the 1st position, the impact is very high, whereas when the turning vehicle is after the 9th position, the impact is low or negligible. Considering equally likely positions from 1 to 11 for the turning vehicle in the same case, the expected performances are shown using solid lines. This reflects the long-term performance of a vehicle when it makes a right turn per cycle. In this case, the expected fuel consumption per vehicle is 12.29 mL under the coordinated system, a significantly lower value than the traditional system, which consumes 15.10 mL, resulting in an 18.56% reduction by the proposed scheme. Furthermore, the expected speed increases to 41.75 km/h under the proposed coordination scheme, which is significantly higher than the traditional one, yielding 35.82 km/h, resulting in a 16.55% speed improvement.

Finally, the performance of vehicles under various traffic flow conditions (moderate to high volume, without exceeding capacity) from both sides with asymmetric flows is investigated. In this case, the probabilistic position of a turning vehicle, along with its corresponding expected velocity and fuel consumption, is considered. Fig. 10 compares the average velocity for different West traffic volumes while keeping a fixed East traffic volume at 315 and 405 veh/h, respectively. In each, fixing the traffic volume on one side and varying it on the other side is an easy way to better understand the influences of traffic demand from each side. As the traffic flow volume increases, the traditional scheme shows a worsening trend, whereas the proposed scheme shows a similar velocity profile. Even for the highly asymmetric flow cases, e.g., 315 veh/h from the East with 540 veh/h from the West, a similar pattern is observed. Overall, as shown by the solid line, the performance improvement varies from approximately 8% to 15% for low to high traffic volumes.

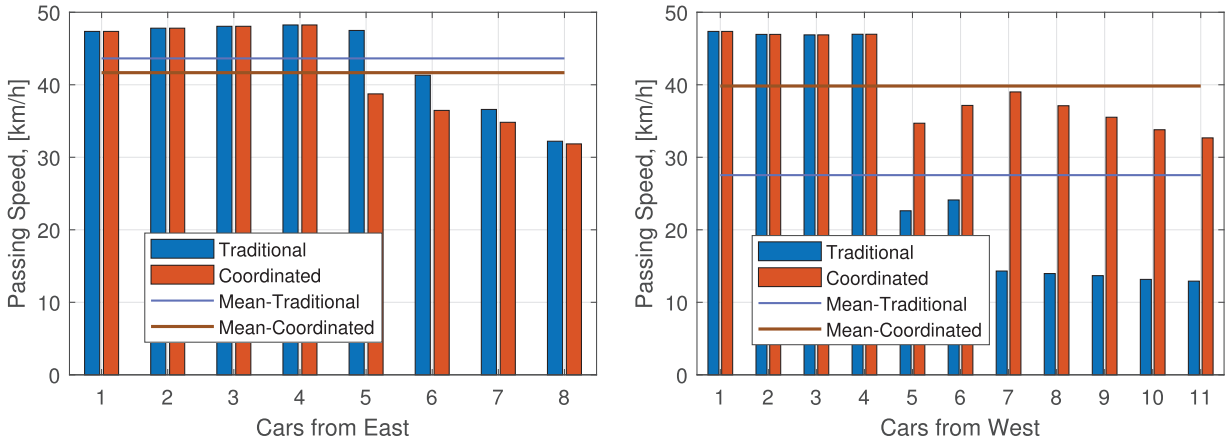

(a) The average speed of individual vehicles from the East and the West.

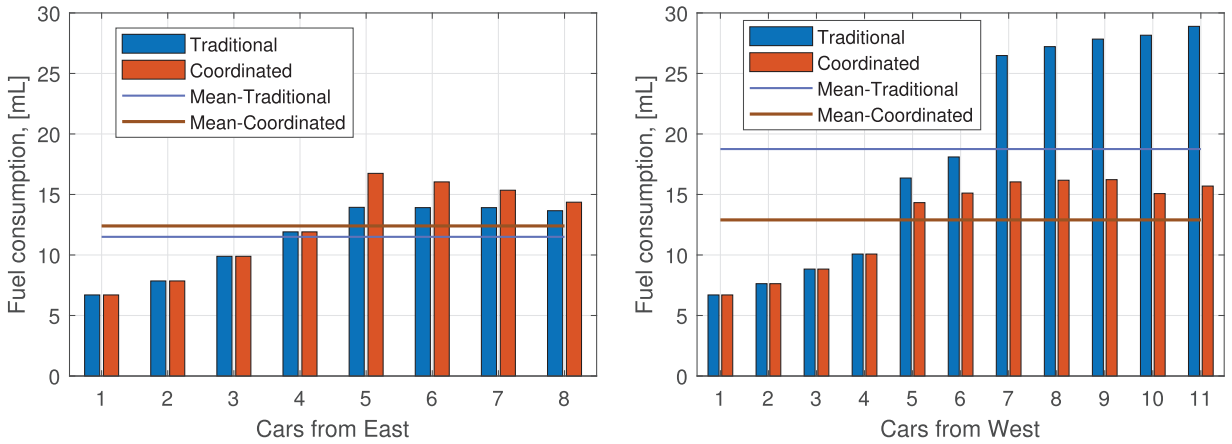

(b) The average fuel consumption of individual vehicles from the East and the West

Figure 8: Comparison of average speed and fuel consumption of individual vehicles under traditional and coordinated systems. The dashed lines show the respective averages of all vehicles

Fig. 11 shows similar trends for fuel consumption improvement. Although the difference in average fuel consumption is low at low traffic volumes between the traditional and coordinated traffic, it becomes significant at higher traffic volumes. Specifically, higher traffic from the East increases the likelihood of blocking many vehicles from the West, thereby worsening the fuel consumption performance. In such a high East traffic scenario, coordination improves fuel consumption by 9%–12%.

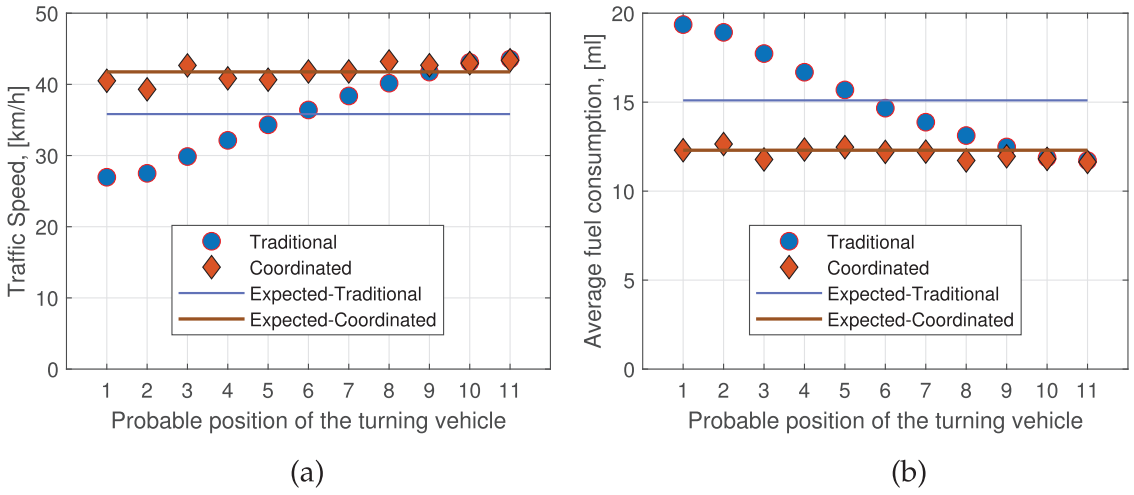

Figure 9: The position of the turning vehicle in a queue of size 11 from the West, and the corresponding all vehicle performances: (**a**) Speed, and (**b**) Fuel consumption. Corresponding expected values are shown using solid lines

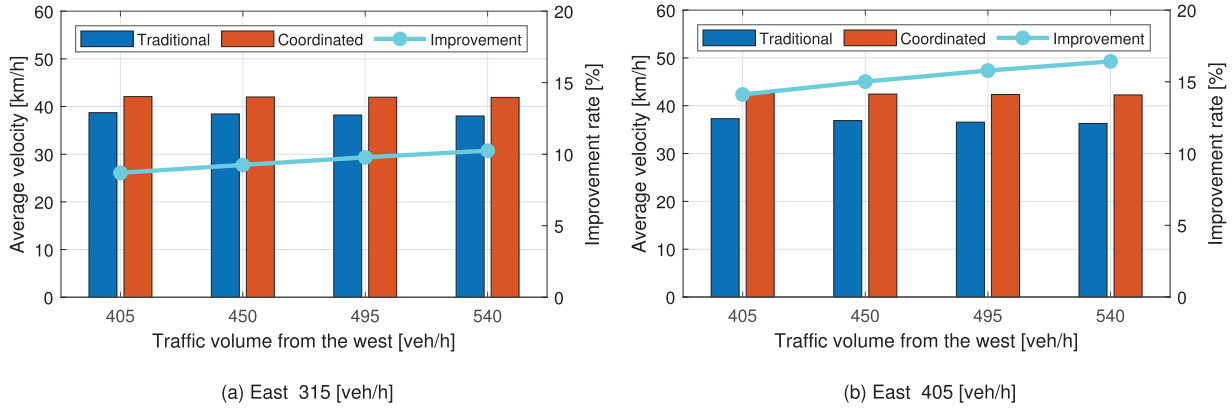

Figure 10: Comparison of average velocity with asymmetric traffic flow variations from the West and the East, with improvements given by solid lines

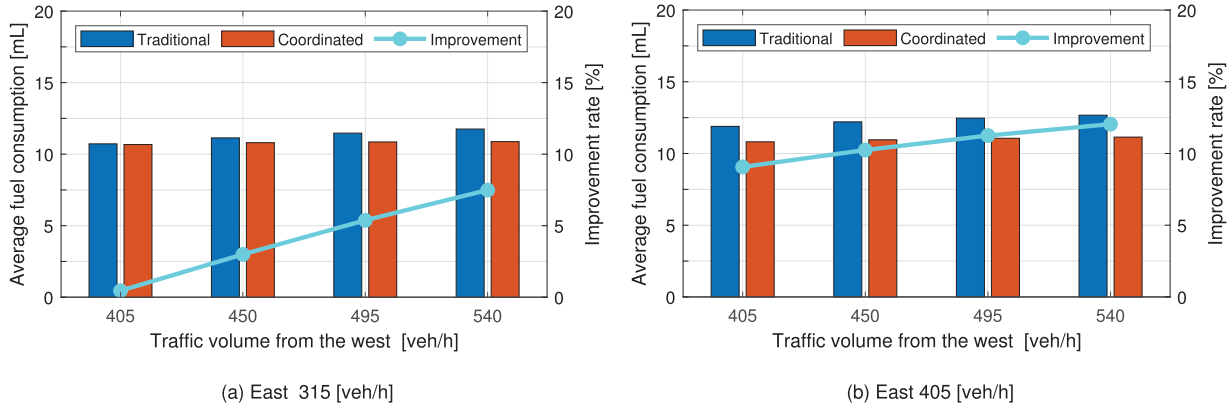

Figure 11: Comparison of average fuel consumption with asymmetric traffic flow variations from the West and the East, with improvements given by solid lines

3.3 Discussion

The computation time of any optimization scheme is crucial. In a brute-force approach, all possible distinct candidate solutions are evaluated to determine the best one without repetitions. However, since the number of constraints depends on the relative positions of the turning vehicles, the computation time primarily depends on the number of affected vehicles, i.e., those that arrive at the same time or later. For the core optimization, which requires the estimated arrival times of all cars, the computation takes only about 4 to 8 ms for the problems considered in this study. In practical applications, vehicles transmit their estimated arrival times directly to the Intersection Control Unit (ICU). Considering a latency of about 50 to 300 ms (based on our Local 5G V2X communication experiments) and an optimization computation time of less than 10 ms, the entire decision-making process can be completed within 500 ms, and feedback to the vehicles can be completed within one second.

Another notable advantage of the proposed scheme is that it requires coordination only once per cycle. After this initial coordination, the vehicles operate independently using their local controllers to ensure safety. Each vehicle is controlled in a distributed manner, allowing for safe operation. Since coordination occurs only once, in unavoidable situations, such as lane blockages, pedestrian crossings, or the need to prioritize emergency vehicles, the system defaults to uncoordinated local driving regulations.

Finally, the limitations of this work should be acknowledged, as we primarily focus on developing an optimal coordination mechanism under ideal traffic and communication conditions, i.e., with minimal driving uncertainty and no communication delay or packet losses. For a human-driven vehicle with connectivity, it may be possible to provide a speed advisory to adjust the arrival at the intersection. Still, such a system may provide better performance than an uncoordinated system, as the vehicle may slow down early instead of going fast and idling. Therefore, such a study is left for future work in this paper.

4 Conclusion

In this paper, we have developed an optimal driving coordination system for CAVs to mitigate traffic congestion resulting from right-turning vehicles on single-lane intersections. Operating within a connected vehicle framework, the system enables the real-time exchange of critical information with an ICU that uses this data to recommend optimal crossing or turning times directly to vehicles. The proposed vehicle coordination system is evaluated at a typical urban intersection, and the performance of vehicles is compared to that of traditional, priority-based, uncoordinated traffic systems. Microscopic traffic simulation results show that the proposed coordination system significantly improves the average traffic speed and fuel consumption compared to the traditional traffic system in various scenarios. Specifically, by precisely optimizing right-turn timing to minimize a quadratic objective function, the ICU effectively reduces waiting times for right-turning vehicles, resulting in lower overall traffic delays and improved fuel efficiency. Further analysis of vehicle positioning under various conditions and expected outcomes supports these benefits.

Future work will focus on refining the optimization algorithms by addressing communication challenges, such as latency, missing data, and partial connectivity. Additionally, integrating various traffic factors can enhance the applicability of the proposed scheme in different urban environments and driving scenarios, particularly in managing multiple turning vehicles approaching from both directions and their priority. Moreover, Artificial Intelligence-based algorithms can be an interesting future work to handle more complex scenarios that are difficult to model as an optimization problem.

Acknowledgement: The authors would like to thank the Center for Research on Adoption of NextGen Transportation Systems, Mabashi, Gunma, for their support.

Funding Statement: This research is supported by the Japan Society for the Promotion of Science (JSPS) Grants-in-Aid for Scientific Research (C) 23K03898.

Author Contributions: The authors confirm their contribution to the paper as follows: Conceptualization, Mahmudul Hasan, Shuji Doman, and Md Abdus Samad Kamal; methodology, Mahmudul Hasan and Md Abdus Samad Kamal; software, Shuji Doman; formal analysis, Mahmudul Hasan, A. S. M. Bakibillah; data curation, Shuji Doman and Mahmudul Hasan; writing—original draft preparation, Mahmudul Hasan and Shuji Doman; writing—review and editing, A. S. M. Bakibillah, Md Abdus Samad Kamal, and Kou Yamada; supervision, A. S. M. Bakibillah, Md Abdus Samad Kamal, and Kou Yamada; project administration, Md Abdus Samad Kamal and Kou Yamada; funding acquisition, Md Abdus Samad Kamal. All authors reviewed the results and approved the final version of the manuscript.

Availability of Data and Materials: Not applicable.

Ethics Approval: Not applicable.

Conflicts of Interest: The authors declare no conflicts of interest to report regarding the present study.

References

1. Rahman MM, Najaf P, Fields MG, Thill JC. Traffic congestion and its urban scale factors: empirical evidence from American urban areas. Int J Sustainable Transp. 2022;16(5):406–21. doi:10.1080/15568318.2021.1885085.
2. Guo Y, Liu P, Wu Y, Chen J. Evaluating how right-turn treatments affect right-turn-on-red conflicts at signalized intersections. J Transp Saf Secur. 2020;12(3):419–40. doi:10.1080/19439962.2018.1490368.
3. Jayson T, Bakibillah ASM, Tan CP, Kamal MAS, Monn V, Imura J. Electric vehicle eco-driving strategy at signalized intersections based on optimal energy consumption. J Environ Manage. 2024;368:122245. doi:10.1016/j.jenvman.2024.122245.
4. Garcia MHC, Molina-Galan A, Boban M, Gozalvez J, Coll-Perales B, Şahin T, et al. A tutorial on 5G NR V2X communications. IEEE Commun Surv Tutor. 2021;23(3):1972–2026.
5. Kamal MAS, Tan CP, Hayakawa T, Azuma SI, Imura JI. Control of vehicular traffic at an intersection using a cyber-physical multiagent framework. IEEE Trans Ind Inform. 2021;17(9):6230–40. doi:10.1109/tii.2021.3051961.
6. Mahbub AI, Malikopoulos AA, Zhao L. Decentralized optimal coordination of connected and automated vehicles for multiple traffic scenarios. Automatica. 2020;117:108958. doi:10.1016/j.automatica.2020.108958.
7. Miculescu D, Karaman S. Polling-systems-based autonomous vehicle coordination in traffic intersections with no traffic signals. IEEE Trans Automatic Control. 2019;65(2):680–94. doi:10.1109/tac.2019.2921659.
8. Li J, Peng L, Hou K, Tian Y, Ma Y, Xu S, et al. Adaptive signal control and coordination for urban traffic control in a connected vehicle environment: a review. Digital Transp Saf. 2023;2(2):89–111.
9. Namazi H, Taghavipour A. Traffic flow and emissions improvement via vehicle-to-vehicle and vehicle-to-infrastructure communication for an intelligent intersection. Asian J Control. 2021;23(5):2328–42. doi:10.1002/asjc.2508.
10. Galvão G, Vieira M, Vieira M, Vestias M, Vieira P, Louro P. Optimizing urban intersection management: a visible light communication approach for cooperative trajectories and traffic signals. In: Real-time processing of image, depth, and video information 2024. Bellingham, WA, USA: SPIE; 2024. Vol. 13000, p. 63–80. doi:10.1117/12.3016816.
11. Sun G, Zhang Y, Yu H, Du X, Guizani M. Intersection fog-based distributed routing for V2V communication in urban vehicular ad hoc networks. IEEE Trans Intell Transp Syst. 2019;21(6):2409–26. doi:10.1109/tits.2019.2918255.
12. Wang T, Zhao J, Li P. An extended car-following model at un-signalized intersections under V2V communication environment. PLoS One. 2018;13(2):e0192787. doi:10.1371/journal.pone.0192787.
13. Farkas Z, Mihály A, Gáspár P. Analysis of model predictive intersection control for autonomous vehicles. Periodica Polytechnica Transp Eng. 2023;51(3):209–15. doi:10.3311/pptr.22082.
14. Xu B, Ban XJ, Bian Y, Li W, Wang J, Li SE, et al. Cooperative method of traffic signal optimization and speed control of connected vehicles at isolated intersections. IEEE Trans Intell Transp Syst. 2018;20(4):1390–403. doi:10.1109/tits.2018.2849029.

15. Yang B, Obana T, Wang Z, Kaizuka T, Sugimachi T, Sakurai T, et al. Evaluations of different human machine interfaces for presenting right-turn timing at intersections. Int J Intell Transp Syst Res. 2021;19:71–82. doi:10.1007/s13177-020-00223-4.
16. Sun C, Leng J, Lu B. Interactive left-turning of autonomous vehicles at uncontrolled intersections. IEEE Trans Autom Sci Eng. 2022;21(1):204–14. doi:10.1109/tase.2022.3227964.
17. Mahler G, Vahidi A. An optimal velocity-planning scheme for vehicle energy efficiency through probabilistic prediction of traffic-signal timing. IEEE Trans Intell Transp Syst. 2014;15(6):2516–23. doi:10.1109/tits.2014.2319306.
18. Bento LC, Parafita R, Rakha HA, Nunes UJ. A study of the environmental impacts of intelligent automated vehicle control at intersections via V2V and V2I communications. J Intell Transp Syst. 2019;23(1):41–59. doi:10.1080/15472450.2018.1501272.
19. Committee ORADO. Taxonomy and definitions for terms related to driving automation systems for on-road motor vehicles. Warrendale, PA, USA: SAE International; 2021. J3016_202104.
20. Treiber M, Hennecke A, Helbing D. Congested traffic states in empirical observations and microscopic simulations. Phys Rev E. 2000;62(2):1805. doi:10.1103/physreve.62.1805.
21. Kamal MAS, Mukai M, Murata J, Kawabe T. Ecological driving based on preceding vehicle prediction using MPC. IFAC Proc Volumes. 2011;44(1):3843–8. doi:10.3182/20110828-6-it-1002.02748.
22. Kamal MAS, Mukai M, Murata J, Kawabe T. Ecological vehicle control on roads with up-down slopes. IEEE Trans Intell Transp Syst. 2011;12(3):783–94. doi:10.1109/tits.2011.2112648.